Continuously observing the spectrum of a dynamically decoupled spin-1 quantum gas

R. P. Anderson,[1] M. J. Kewming,[1] and L. D. Turner[1]

[1]*School of Physics & Astronomy, Monash University, Victoria 3800, Australia.*
(Dated: June 7, 2017)

Quantum states and spectra can be made sensitive to a particular measurand whilst simultaneously impervious to parasitic fluctuations of an environment. Here we use an atom-light interface with minimal backaction to probe the spectrum of a radiofrequency-dressed spin-1 quantum gas continuously and in-situ. The dressing amplitude sets the radiofrequency band in which oscillating magnetic fields manifest a linear measurand, and we probe the energy spectrum while the system evolves unitarily. By varying a symmetry-breaking parameter of the Hamiltonian, we find a regime in which two of the dressed states are maximally insensitive (up to fourth-order) in magnetic field fluctuations that are slow compared to the dressed-state splittings. Moreover, we demonstrate the predictive power of our continuous probe to optimize the dynamical decoupling and tune the measurement band. This robust system shares the useful hallmarks of quantum metrology platforms; the states are thus termed "synthetic clock" states in a co-published result by Lundblad *et al.* (Phys. Rev. Lett. **118**, 2xxxxx (2017)) and are candidates for band-tunable magnetometry and color charge analogues in quantum gases.

INTRODUCTION

- Minimally insensitive states in other systems, e.g. $|F = 1, m = -1\rangle \leftrightarrow |F = 2, m = +1\rangle$ at $B = 3.23\,\text{G}$ [1], clocks.

- Wide utility of these states for clocks, magnetometers (including microwave, e.g. Treutlein), quantum information, and quantum emulation, e.g. elusive many-body spin-singlet state which requires unforgiving field stability.

- General message of making the eigenspectrum insensitive to one thing while retaining sensitivity to another, and dynamical decoupling in this context. [Are the synthetic clock states an example of a *protected qubit subspace* [1]?]

- In electronically/magnetically sensitive spin experiments, magnetic field noise manifest as small perturbations $\Delta\hat{F}_z$ which shift the energy eigenvalues. Continuous dynamical decoupling (CDD) [1, 2] occurs when the spin undergoes rotations in a plane perpendicular induce perturbation, i.e $\hat{F}_x$ or $\hat{F}_x$ most readily achieved through Rabi coupling where $\Omega \gg \Delta B$. Decoupling can be used to increase the coherence time of single qubits [3] which can be extended even further by doubly dressing the system and decoupling from noise induced by the first coupling field [4]. It has also been shown theoretically that CDD is superior than pulsed sequence dynamical decoupling for single solid-state qubits for magnetometery [5]. [There is a wealth of literature on this topic in NV. Should trace down the biggest results in this field and cite them [6].]

- Motivate continuous measurement, especially in context of measurement bandwidth; it doesn't make sense to measure something in kHz–MHz
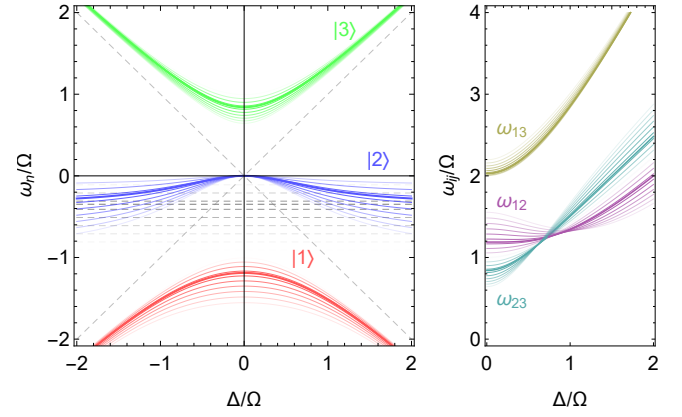

FIG. 1. (Color online) Energy spectrum and splittings of a radiofrequency coupled spin-1 for various $q(B) \in [0, \Omega]$. The transparency of each curve is proportional to the distance of the quadratic shift q from $q_{\text{magic}} \approx 0.348\Omega$. (Left) Energies ω_n of dressed states $|n\rangle = |1\rangle$, (red) $|2\rangle$ (blue), and $|3\rangle$ (green) normalized to the rf-coupling strength (Rabi frequency) Ω as a function of detuning $\Delta(B) = \omega_{\text{rf}} - \omega_L(B)$, Dashed lines indicate the energies of uncoupled states ($\Omega = 0$) in a frame rotating at ω_{rf}. (Right) Splittings ω_{ij} of dressed states $|i\rangle$ and $|j\rangle$ as a function of detuning. When $q = q_{\text{magic}}$ (bold curves), energies ω_1 and ω_2 share the same curvature, and their difference ω_{12} (right, purple) is minimally sensitive to detuning and thus magnetic field variations.

band using a shot-based (0.1 Hz or less) readout. Why? Can't react, can't feedback, can't always assume periodicity/repeatability.

- Whilst the paper is not focused on introducing spectrograms, we can say they provide a new mechanism for appraising spectrum of a quantum system in real-time.

- From a magnetometry perspective, breaking rota-

tional symmetry is bad because you want there to be no anisotropy to the sensitivity. How does this relate to this work?

- [Not sure about this but many NV center guys study Luminescence as a function of time. Could they make spectrograms with there data? See data from [4].]

- (How) The $\hat{F}_z^2$ interaction has been controlled using static magnetic fields, microwave ac Stark shifts and tensor-light shifts of off-resonant magnetic and electric dipole transitions, respectively. In collective psuedo-spins, it can arise from nonlinear collisional interactions [7].

- (What) This nonlinear term has been used to traverse the magnetic phase space of a spinor quantum gas, drive quantum quenches of same, initiate spin dynamics in optical lattices [8], enact the canonical spin-squeezing of Kitagawa and Ueda [9]: one-axis twisting (shear of coherent spin state uncertainty regon) that has squeezed atomic spins in cavities [10], Bose-Einstein condensates [7], and superconducting qubits.

Continuous measurement using the linear Faraday effect:

- Paramagnetic Faraday effect has been used to continuously measure spin-mixing dynamics of a polar spinor condensate [11].

- Quantum state tomography (QST) [12] using continuous weak measurement and dynamical control. Ref. [12, 2004] foreshadows "real-time estimation of the spin density matrix" via weak measurement.

- Real-time nonperturbing polarization probe (tensor-based at $\Delta \sim \Delta_{HF}$, not Faraday) in Ref. [13] measured hyperfine Rabi oscillations of the collective clock-transition pseudospin. The birefringence is modulated near baseband, i.e. polarization rotation oscillates at the Rabi frequency. This paper highlights the fact that "atoms in $m_F = 0$ clock states cannot contribute to Faraday rotation, and therefore in the limit $\Delta \gg \Delta_{HF}$ the probe polarization does not couple to the clock pseudospin". In contrast, the synthetic clock states presented here can yield Faraday rotation, including in the $\Delta \gg \Delta_{HF}$ limit. Moreover, the probe-induced differential light shift changed the resonance of the clock-transition (detected as a modified total Rabi frequency). Also from this paper:

  > ...if a measurement can resolve the quantum fluctuations associated with a collective observable, then backaction will be induced on the collective state and the observable can be squeezed.

- Faraday QND measurement of collective spin projection of an atomic beam as a way of preparing squeezed spin states [14]. This is an odd regime where the background field is modulated faster than the peak Larmor frequency, but it is a rare example of the polarimetry signal being fed to a spectrum analyzer/lock-in detector.

Other exotica:

- Spin-orbit coupled spin-1 Bose gases exhibit e.g. tricriticality in (Ω, q) phase diagrams [15], where the optimal decoupling $q = q_{R,\text{magic}}\Omega$ is a line traversing multiple phases, in the vicinity of a tricritical point of polar-striped and plane-wave phases. Although here the wavevector of the coupling is zero, the essential results may carry over, and the Faraday probe – used to detect magnetization – could constitute one of the Raman beams used to generate the spin-orbit coupling.

- Lipkin-Meshkov-Glick Hamiltonian [16] (see Refs. [16] of [17]).

BACKGROUND + RANDOM

Hamiltonians (quasi-static field along z, coupling field along x:

$$\hat{H}_{\text{lab}} = -\omega_L \hat{F}_z + q\hat{F}_z^2 - 2\Omega\cos(\omega_{\text{rf}}t)\hat{F}_x$$
$$\Rightarrow \hat{H}_{\text{rwa}} = \Delta\hat{F}_z + q\hat{F}_z^2 + \Omega\hat{F}_x \,, \text{ where}$$
$$\omega_L(B) \equiv (E_{m=-1} - E_{m=+1})/2\hbar \,, \text{ and}$$
$$q(B) \equiv (E_{m=+1} + E_{m=-1} - 2E_{m=0})/2\hbar$$

are the Larmor frequency and quadratic shift, respectively, which can be gleaned from the Breit-Rabi equation. The rf Rabi frequency $\Omega = \gamma B_{\text{rf}}/2$ and detuning $\Delta(B) = \omega_{\text{rf}} - \omega_L(B)$.

The control field $\mathbf{B}(t \geq 0) = -B_{\text{rf}}\cos(\omega_{\text{rf}}t)\mathbf{e}_x + B_z(t)\mathbf{e}_z$, where $B_z(t) = B_0 + \alpha t + B_{\text{ac}}(t)$ is the sum of a linear ramp and parasitic power-line magnetic noise.

- At low magnetic field strengths, $\omega_L \propto B$ and $q \propto B^2$, and for our parameters we are justified in taking $\omega_L = \gamma B$ and $q = q_Z B^2$, where $\gamma = 2\pi \times 702.379\,\text{kHz/G}$ is the gyromagnetic ratio for ^{87}Rb $F = 1$ and $q_Z = 2\pi \times 71.89\,\text{Hz/G}^2$.

- For most of the analysis presented here (with ω_L and q defined as above) these proportionalities need not be met, or the results, e.g. value of q_{magic} require a small correction.

- For $q = 0$, $\hat{H}_{\text{lab}}$ and $\hat{H}_{\text{rwa}} \propto \mathbf{B} \cdot \hat{\mathbf{F}}$ and are thus a generator of rotations, but $q\hat{F}_z^2 \neq 0$ breaks the SU(2) symmetry and $\langle\hat{\mathbf{F}}\rangle^2$ is not preserved.
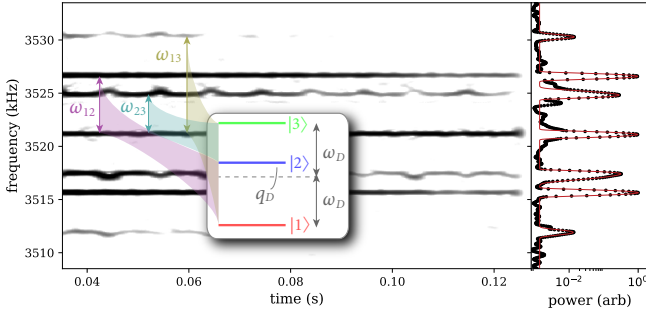
FIG. 2. Continuous measurement of the dressed energy spectra for $q_R = 0.402(3)$, $f_{rf} = 3.521\,\mathrm{MHz}$ and $B_0 = 5.013\,\mathrm{G}$ (left) and the log of the fitted moving average signal strength in normalized units (right). The shape of the energy spectra in the Fourier domain are Gaussian, but magnetic field fluctuations skew the time average shape. Skewed Gaussian curves are fitted to each peak resulting in a significant skew parameter of $\gamma = 2.4(1)$ for the ω_{23} splitting width $\sigma_{23} = 243(2)\,\mathrm{Hz}$. The fit of the transition most decoupled from magnetic field fluctuations ω_{12} has a vanishing skew and is well approximated by a Gaussian of width $\sigma_{12} = 109(1)\,\mathrm{Hz}$.

- This broken symmetry lifts the degeneracy of the dressed state splittings making them distinguishable in our spectrogram measurements.

- We vary the magnetic field to affect a change in the detuning of $\Delta \in [0, 2\Omega]$, the domain of Fig. 1(B).

- Variations in $B \mapsto B_0 + \Delta B$ of order $B_{rf} = 2\Omega/\gamma$ affect the detuning linearly, $viz.$ $\Delta = -\gamma \Delta B$ for $\omega_L(B_0) = \omega_{rf}$ (i.e. rf is resonant when $B = B_0$), and do not affect q appreciably for sufficiently small field strengths.

- Indeed, our data corroborate this since we measure $q(B(t))$ across the calibration sweep and find that $\sigma(q)/(2\pi) = 11.7\,\mathrm{Hz}$ on average (alternatively, inferring q from ω_L via Breit-Rabi gives $\sigma(q)/(2\pi) = 1.2\,\mathrm{Hz}$).

- Thus the horizontal axis Δ/Ω in Fig. 1 is a proxy for ΔB, and ω_{12} at $q = q_{magic}$ has leading-order quartic sensitivity to ΔB.

- At high fields ($B \approx 30\,\mathrm{G}$) this approximation is no longer valid; $q \approx q_{magic}$ varies appreciably across $\Delta B \in [0, B_{rf}]$ and ω_{12} has weak linear dependence on ΔB [18].

- *On varying Ω or q to change $q_R = q/\Omega$:* For a given static magnetic field, q_R can be modified via the Rabi frequency. However, this is not what is represented in Fig. 1, as the normalization of the horizontal and vertical axes would vary for each q_R. Importantly, the insensitivity of ω_{12} to detuning only gets better for increasing Ω in absolute terms; if the rf amplitude is unlimited, use it. However,
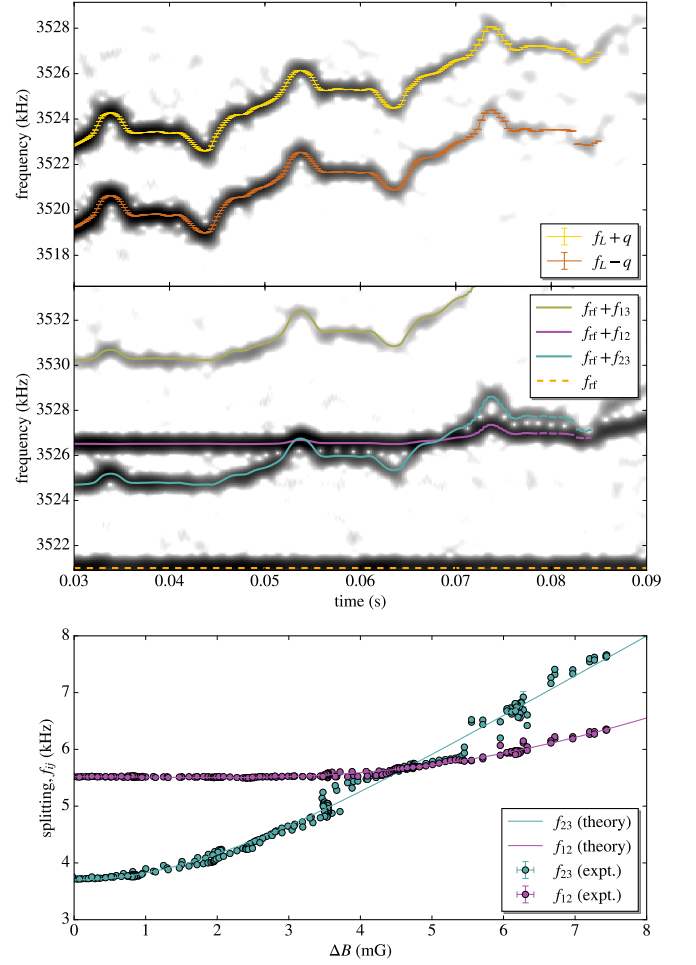

FIG. 3. (Color online) Acquisition and analysis pipeline of the continuous spectrum observation for $q_R = 0.402(3)$ ($f_{rf} = 3.521\,\mathrm{MHz}$, $B_0 = 5.013\,\mathrm{G}$). The underlay of (A) and (B) are spectrograms of raw acquisitions from the polarimeter measuring Faraday rotation of the probe beam. (A) Time-resolved magnetometry is used to calibrate the instantaneous magnetic field $B(t) = B_0 + \Delta B(t)$ over the interrogation interval, in which the field [detuning] varies over a range $\sim B_{rf}$ [2Ω] and the spinor gas is left to Larmor precess in the absence of a dressing field. We fit sinc peaks in the frequency domain for each spectrogram window (time domain) to determine $f_L(t)$ and $q(t)$. (B) The field is swept over the same range but the radiofrequency dressing is applied. Three sidebands appear above (shown) and below the carrier at f_{rf} (dashed, orange), revealing the dressed state splittings ω_{ij}. (C) A parametric plot of $\omega_{12}(t)$ and $\omega_{23}(t)$ versus $\Delta B(t)$ by combining analysis of (A) and (B). Solid curves in (B) and (C) are theoretical splittings from an eigenspectrum calculation, provided only f_{rf}, $B(t)$, and Ω, i.e. no free parameters.

doing so also modifies the absolute dressed state splittings on resonance, and thus the bandwidth of the dressed spin-1 as an ac magnetometer. The take home message is then: use as high an rf amplitude as you can afford (or want to tune the ac-band to), and then modify q_R via q to realize the

synthetic clock states.

- *Transitions between dressed states:* $|1\rangle \leftrightarrow |2\rangle$ and $|2\rangle \leftrightarrow |3\rangle$ driven by fields oscillating along y or z near frequencies $\omega_D \mp q_D$, respectively. Alternatively, $|1\rangle \leftrightarrow |3\rangle$ driven by fields oscillating along x near frequency $2\omega_D$. This is very different to the fully polarized bare states $|m = \pm 1\rangle$, which are coupled by a single-photon transition as this would conserve neither photon number nor angular momentum. There is no such restriction on the dressed states however as they are neither eigenstates of $\hat{F}_z$ nor photon number.

Lab frame eigenstates:

- mean splitting ω_L; quadratic shift q.

- Pairwise coupling between $|m = -1\rangle \leftrightarrow |m = 0\rangle$ and $|m = 0\rangle \leftrightarrow |m = +1\rangle$ via $\hat{F}_x$ and/or $\hat{F}_y$, i.e. affected by fields transverse to the static field oscillating near ω_L.

Dressed states on resonance:

- Dressed Larmor frequency:

$$\omega_D \equiv (\omega_3 - \omega_2)_{\Delta=0}/2 = (\omega_{12} + \omega_{23})_{\Delta=0}/2$$
$$= \sqrt{\Omega^2 + q_D^2}\,.$$

- Dressed quadratic shift:

$$q_D \equiv (\omega_3 + \omega_1 - 2\omega_2)_{\Delta=0}/2$$
$$= (\omega_{23} - \omega12)_{\Delta=0}/2$$
$$= -q/2\,.$$

- Thus $\Omega = \sqrt{\omega_{12}\omega_{23}}_{\Delta=0}$ and $q_D = (\omega_{23}-\omega_{12})_{\Delta=0}/2$, both of which can be attained from the dressed sideband splittings on resonance. Such high-bandwidth measurement of Ω (magnetic field oscillating along x with amplitude $B_{\rm rf}$ and frequency ω_L) allows (in principle) closed-loop control of Ω using the atoms.

- For $q = 0$ (low-field limit), the dressed states at $\Delta = 0$ are eigenstates of $\hat{F}_x$, and: (i) the spectrum has vanishing linear sensitivity to magnetic fields, with the leading quadratic sensitivity (as in spin-1/2), and (ii) fields along y or z oscillating near the Rabi frequency Ω drive transitions between different $|m_x\rangle$ states. [Cite other dressed-ception papers on both of these.]

- Curvature of the dressed-state energies can be evaluated using perturbation theory;

$$\frac{\partial^2 \omega_n}{\partial \Delta^2} = \sum_{k \neq n} \frac{|\langle k|\hat{F}_z|n\rangle|^2}{\omega_n - \omega_k}\,.$$

- Thus the curvature of the dressed-state splittings can be found. In particular, the dimensionless curvature of ω_{12} is (presuming $|\partial q/\partial \Delta| \ll 1$)

$$\frac{\partial^2(\omega_{12}/\Omega)}{\partial(\Delta/\Omega)^2} = \Omega \frac{\partial^2 \omega_{12}}{\partial \Delta^2}$$
$$= -\frac{3q_R\sqrt{4 + q_R^2} - q_R^2 - 2}{2\sqrt{4 + q_R^2}}\,.$$

This vanishes when $q = q_{R,\rm magic}$, given by

$$q_{R,\rm magic} = \sqrt{(3\sqrt{2} - 4)/2} \approx 0.348\,.$$

For $q_R = 0$, we recover the spin-1/2 result, $\Omega\,\partial^2\omega_{12}/\partial\Delta^2 = 1$.

- Similarly, perturbation theory can be used to show that the third-order derivatives of ω_n with respect to detuning all vanish when $|\partial q/\partial \Delta| \approx |\gamma^{-1}\partial q/\partial B| \ll 1$, and thus the leading sensitivity to detuning (and thus B) is fourth-order. This validates the choice of our phenomenological even-polynomial model for fitting to $(\Delta B(t), \omega_{12}(t))$ data extracted from Faraday spectrograms.

- The above can be quantified by noting that $\gamma^{-1}\partial q/\partial B = 2Bq_Z/\gamma \lesssim 10^{-3}$ for $B \lesssim 5\,\rm G$.

- Near $q = q_{\rm magic}$, the ratio of the Rabi frequency to the Larmor frequency is approximately:

$$\frac{\Omega}{\omega_L} = \frac{B_{\rm rf}}{B_0}$$
$$\approx \frac{q_z B_0}{\sqrt{2}\gamma\, q_{R,\rm magic}}$$
$$= 2.1 \times 10^{-4} B_0\,,$$

with B_0 is in Gauss. Thus for $B_0 \lesssim 5\,\rm G$, $\Omega/\omega_L \lesssim 10^{-3}$ and the rotating-wave approximation is justified.

- For $0 \leq \Delta B \leq B_{\rm rf}/4 = 3.2\,\rm mG$ ($0 \leq |\Delta/\Omega| \leq 0.5$) we observe a variation in the splitting f_{12} of $39\,\rm Hz$ for the data in Fig. 3, compared to the theoretical estimate of $26\,\rm Hz$. These correspond to a normalized variation in ω_{12}/Ω of 8.6×10^{-3} and 5.8×10^{-3}, respectively. By comparison, the normalized variation at $q_R = 0$ is $(\sqrt{5} - 2)/2 \approx 0.118$; 14 [20] times higher than the observed [predicted] variation. Alternatively, the normalized variation of the $|m = \pm 1\rangle \leftrightarrow |0\rangle$ transitions at $q = 0$ is 0.5; 58 [86] times higher than the observed [predicted] variation in the synthetic clock transition frequency. [Both of these comparisons depend a lot on the range of ΔB! They are far more impressive (theoretically) for smaller ranges.]

TABLE I. Upper sidebands of the carrier (at ω_{rf}) of the Faraday rotation signal $\propto \langle \hat{F}_x \rangle$ of a state $|\psi(t=0)\rangle = |m=1\rangle$ driven on resonance ($\Delta = 0$) in the laboratory frame. Frequency and phase are reported relative to the carrier, along with the transition that each sideband corresponds to. For each upper sideband, there is a lower sideband of the same amplitude, relative frequency and opposite [π] relative phase.

frequency	amplitude	transition
0	$\frac{q_D \Omega}{2\omega_D^2}$	$-$
$\omega_D - q_D$	$\frac{\Omega}{4\omega_D}$	$|1\rangle \leftrightarrow |2\rangle$
$\omega_D + q_D$	$\frac{\Omega}{4\omega_D}$	$|2\rangle \leftrightarrow |3\rangle$
$2\omega_D$	$\frac{q_D \Omega}{4\omega_D^2}$	$|1\rangle \leftrightarrow |3\rangle$

- The $F=1$ spin operators in the undressed basis do not span all of SU(3), i.e. $\sigma_x = (\lambda_1 + \lambda_6)/\sqrt{2}$, $\sigma_y = (\lambda_2 + \lambda_7)/\sqrt{2}$, and $\sigma_z = (\lambda_3 + \sqrt{3}\lambda_8)/2$ (λ_4 and λ_5 which include off diagonal terms in rows/columns 1 and 3 are absent) where $\lambda_i, i = 1, \ldots, 8$ are the Gell-Mann matrices.

- The $F=1$ spin operators in the dressed basis span [almost] all of SU(3), as $[\hat{F}_x]_D = (q_D/\omega_D)Q_{x^2-y^2} - (\Omega/\omega_D)\sigma_z = (q_D/\omega_D)\lambda_4 - \Omega/\omega_D(\lambda_3 + \sqrt{3}\lambda_8)/2$, $[\hat{F}_y]_D$ is a sum of λ_1, λ_2, and λ_7, and $[\hat{F}_z]_D$ is a sum of λ_1 and λ_6. [The spin operators have no projection onto λ_5, even for an rf field oscillating along y.]

Analytic Faraday signal on resonance: The Faraday signal we detect is proportional to $\langle \hat{F}_x \rangle$ in the laboratory frame, which is given by $\langle \psi(t)|\hat{S}^\dagger \hat{F}_x \hat{S}|\psi(t)\rangle$ where $|\psi(t)\rangle = \exp(-i\hat{H}_{\mathrm{rwa}}t/\hbar)|\psi(t=0)\rangle$, and $\hat{S} = \exp(-i\omega_{\mathrm{rf}}\hat{F}_z t)$. For an initially polarized $|\psi(t=0)\rangle = |m=1\rangle$ state driven on resonance, we get

$$\langle \hat{F}_x \rangle_{\mathrm{lab}} = -\frac{\Omega}{\omega_D}\cos(q_D t)\sin(\omega_D t)\sin(\omega_{\mathrm{rf}}t) - \frac{q_D \Omega}{\omega_D^2}\sin^2(\omega_D t)\cos(\omega_{\mathrm{rf}}t).$$

The first term has equal-amplitude sidebands at $\pm(\omega_D \pm q_D)$ and the second term has smaller amplitude sidebands at $\pm 2\omega_D$, as summarized in Table I. The ratio of the ω_{13} sideband amplitude to the ω_{12} and ω_{23}) sideband amplitudes is $q_R/\sqrt{4+q_R^2} \approx 0.197$ for $q_R = 0.402$ in Fig. 3. For the data in Fig. 2 we measure the ratio of sideband amplitudes to be 0.699 and 0.210 of the ω_{23} and ω_{13} peaks relative to the ω_{12} peak respectively.

Faraday signal for arbitray states: Evaluating $\langle \hat{F}_x \rangle_{\mathrm{lab}}$ in the dressed basis, one can show analytically that the sideband frequencies are the dressed state splittings ω_{ij} with amplitudes proportional to the relevant dressed-state coherence $\rho_{ij} = \langle i|\psi\rangle\langle\psi|j\rangle$. The carrier amplitude is $(\rho_{33} - \rho_{11})\Omega/\omega_D$. This explains the relative longevity

of the sidebands; the transition most sensitive to detuning is ω_{13}, and thus the coherence ρ_{13} decays the fastest in the presence of detuning noise. Conversely, the transition least sensitive to detuning ω_{12} exhibits the longest-lived coherence. The spectrogram makes this plain: the sideband with the least frequency modulation lasts the longest. [Can we be quantitative about this, quoting $1/e$ times for Fig. 2 or other data?]

Adiabatic considerations: The rf-dressing is applied non-adiabitcally, and as a result we project $|m=-1\rangle$ onto the dressed basis at the initial detuning $\Delta(t=0)$ into a state

$$\begin{pmatrix} \langle 1|\psi(t=0)\rangle \\ \langle 2|\psi(t=0)\rangle \\ \langle 3|\psi(t=0)\rangle \end{pmatrix} \approx \begin{pmatrix} \frac{1}{\sqrt{4+q_R\left(q_R+\sqrt{q_R^2+4}\right)}} \\ -\frac{1}{\sqrt{2}} \\ \frac{1}{\sqrt{4+q_R\left(q_R-\sqrt{q_R^2+4}\right)}} \end{pmatrix}$$

for $\Delta(t=0) \ll \Omega$. In the adiabatic limit, the dressed state populations remain constant and the above superposition evolves under phase acquisition $e^{-i\omega_i t}$ by each dressed state $|i\rangle$ [19]. We quantify the stasis of the dressed superposition using the generalized adiabatic parameter $\Gamma \equiv |\mathbf{\Omega}(t)/\dot{\theta}(t)|$, where $\mathbf{\Omega} = \mathbf{B}_{\mathrm{eff}}/\gamma \equiv \Omega\,\mathbf{e}_x + \Delta\,\mathbf{e}_x$ and $\tan\theta \equiv \Omega/\Delta$. For constant coupling amplitude $\dot{\Omega} = 0$, $\dot{\theta}(t) = -\Omega\dot{\Delta}(t)/|\mathbf{\Omega}|^2$. For the magnetic field sweeps used here, $\Gamma > 200$ and $\sqrt{\langle\Gamma^2\rangle_t} \gtrsim 600$ where $\langle\cdot\rangle_t$ denotes the time-average over the duration of the sweep. Nevertheless, the continuous spectra when plotted parametrically (Fig. 3(bottom)) exhibit some evidence of non-adiabatic following. This is corroborated by numerically integrating the Schrödinger equation of the known control Hamiltonian; the dressed state populations vary slowly (compared to ω_D^{-1}) but by a few percent near minima of $\Gamma(t)$, i.e. when the sweep is least adiabatic.

APPARATUS

Our spinor quantum gas apparatus [20] and Faraday atom-light interface are described in greater detail elsewhere [21]. We prepare an ultracold gas ($\sim 1\,\mu$K) of approximately 10^6 ^{87}Rb atoms in a crossed-beam optical dipole trap ($\lambda = 1064$ nm). The three Zeeman states $|m=-1,0,+1\rangle$ of the lowest hyperfine ($F=1$) ground state are coupled using a radiofrequency field with $\Omega/(2\pi) \leq 100$ kHz, generated by a single-turn coil placed immediately atop the glass vacuum cell, fed by an amplified radiofrequency source generated using direct-digital synthesis. A component of the spin (e.g. $\langle \hat{F}_x \rangle$) transverse to the static magnetic field direction (along z) rotates the polarization of an off-resonant probe beam via the paramagnetic Faraday effect. By tuning the probe to a magic-zero wavelength at $\lambda = 790.0$ nm, and ensuring it is linearly polarized, the probe exerts no scalar or vector
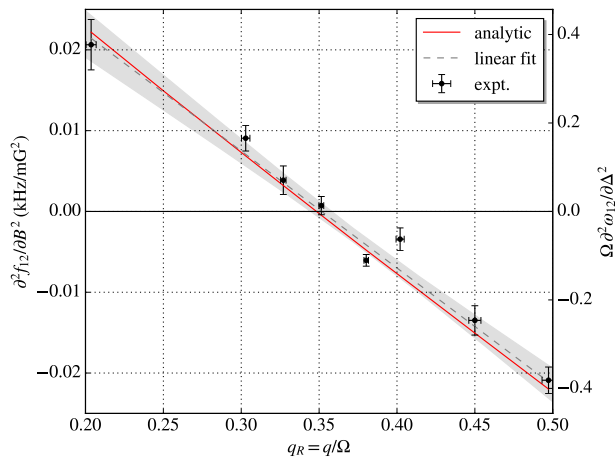
FIG. 4. Curvature of the synthetic clock transition for various quadratic shifts $q_R \in [0.2, 0.5]$. The measured curvature (black points) was determined from polynomial fitting to $(\Delta B, f_{12})$ data shown in Fig. 3(B). Vertical and horizontal error bars correspond to the standard error of the regression and uncertainty in q_R (via $u(q)$ and $u(\Omega)$ at each field B_0), respectively. A linear fit (black, dashed) with 1–sigma confidence band (gray, shaded) are shown, whose intercept can be used to impute $q_{R,\mathrm{magic}}$ (expt.) = 0.350(6). The analytic expression for the curvature (red) is consistent with the data-driven analysis of the curvature, cf. $q_{R,\mathrm{magic}}$ (theory) = 0.348. The left [right] vertical axis shows the curvature $\partial^2 f_{12}/\partial B^2$ [$\Omega \partial^2 \omega_{12}/\partial \Delta^2$] in absolute units of kHz/G^2 [dimensionless units, with the splitting and detuning normalized to the Rabi frequency]. cf. The normalized curvature is unity when $q_R = 0$.

light shift on the atoms. The former would enact a dipole force on the cloud, perturbing its total density, whereas the latter would be manifest as a fictitious magnetic field and gradient, dephasing the collective spin [22]. Here we used a wavelength of $\lambda = 781.15$ nm to increase the SNR with respect to the rf pickup at f_{rf}; the measured $1/e$ decay time of calibration peaks $\tau_s = 23.8(2)$ ms is consistent with scattering in [21] for a 10.6 mW probe with $1/e^2$ diameter of 150 μm (peak intensity $I_0 = 120.1(4)$ W/cm^2).

We detect the Faraday rotation of the probe light using a shot-noise limited balanced polarimeter, with bandwidth up to 8 MHz, and record the signal using an AlazarTech ATS9462 digitizer (16-bit, 180 MS/s) [23]. Upon applying the radiofrequency (rf) dressing field, $|\langle \hat{F}_x \rangle| > 0$ and the signature of the coupled spin-1 system is a Faraday signal frequency modulated (FM) about a carrier at the Larmor frequency. The frequency difference of each FM sideband from the carrier is a calibration-free measure of each dressed state splitting ω_{ij}.

As we seek to appraise the robustness of the rf-dressed states to varying magnetic fields, we apply a time dependent $\Delta B(t)$ and observe the dynamical change in the frequency composition of the Faraday signal using the

short-time Fourier transform, or spectrogram. The time-dependent magnetic field shift $\Delta B(t)$ is the sum of an applied linear ramp and the parasitic background fluctuations at the power-line frequency of 50 Hz and its odd harmonics, and typically ranges from 0 ($\Delta = 0$, resonance) to B_{rf} ($\Delta = 2\Omega$), cf. Fig. 1. For each realization (or 'shot') of the experiment, we directly calibrate this time-dependent field using ac magnetometry; an rf $\pi/2$-pulse (rather than continuous coupling) initiates Larmor precession of the collective spin the x–y plane, and the Faraday signal is composed of two tones, at $\omega_\pm = \omega_L \pm q$. For $q\,\tau_f \geq 2\pi$, where τ_f is the length of the overlapping spectrogram windows, the two tones are spectrally resolved and their mean and difference yields the instantaneous $\omega_L(t)$ and $q(t)$, the former of which is used to find $\Delta B(t)$ by inverting the Breit-Rabi equation [24]. The experiment is synchronized to the AC power line; the harmonic composition of which varies little between contiguous shots (20 s apart), and thus the measured $\Delta B(t)$ and $q(t)$ from the calibration [fiducial?] shot serve as a good proxy for the values experienced by the atoms in the subsequent rf-dressed shot.

We measured the dressed spectrum for a range of $q_R \in [0.2, 0.5]$ by varying the resonant magnetic field B_0 [applied rf frequency f_{rf}] from 3.549 G [2.493 MHz] to 5.568 G [3.911 MHz], with a fixed Rabi frequency of $\Omega/(2\pi) = 4.505(3)$ kHz ($B_{\mathrm{rf}} = 12.83(1)$ mG). For each resonant field B_0, we ensured the Rabi frequency was fixed by measuring the voltage drop across the coil at f_{rf} with a lock-in amplifier which – in concert with an impedance analyzer – could be used to ensure the rf current in the coil and thus B_{rf} and Ω were constant. The Rabi frequency was ultimately measured using the atoms, by analyzing a subset of the dressed energy spectrum during the magnetic field sweep when $|\Delta|/(2\pi) \leq 100$ Hz. The measured Rabi frequencies had a standard deviation $\sigma(\Omega) = 9.4$ Hz, validating the above method.

Despite long coherence times, the low duty cycle ($D < 0.01$) and large dead time ($T_{\mathrm{shot}} \gtrsim 10$ s) of cold quantum gas experiments make challenging achieving metrological sensitivities per unit bandwidth that are competitive with other platforms. Here $D = 0.005$ and $T_{\mathrm{shot}} = 20$ s, yet we make many more spin projection measurements ([N_m = blah] at a shot-noise limited SNR of 10–100 [21]) than traditional cold atom experiments ($N_m = 1$ to several, e.g. absorption or dispersive imaging). This intra-shot revelation of the time and frequency domain renders the measurement of these spectra orders of magnitude more efficient. For example, the single spectrum shown in Fig. 3 would take $\sim$ (10 shots per ΔB per ω_{ij}) × (100 different ΔB values) ×(3 different transition frequencies ω_{ij}) = 3000 shots (2.5 times fewer ΔB values than shown here), or $\sim 6 \times 10^4$ s = 1000 minutes of data acquisition. We acquire this spectrum in a single shot [two shots accounting for the field calibration, but that would require $\sim 2\times$ more traditional shots], i.e. 20 s. The data used to

generate Fig. 4 was acquired in only 6 minutes.

THE DATA - THINK OF SEXIER TITLE

Our technique directly measures all the quantities in the dressed energy eigen spectrum using sinc fitting to the spectrogram data in a two shot experiment. The first observation calibrates essential quantities of the magnetic field $(q_z, \omega_L, \frac{\partial B}{\partial t})$ Fig. 3A characterising the horizontal axis of Fig. 1B. In the second shot, we repeat the experiment but dress the atoms with RF Fig. 3B from which we measure the energy splitting.

[1] M. R. Matthews, Physical Review Letters **81**, 243 (1998); N. Aharon, M. Drewsen, and A. Retzker, Physical Review Letters **111**, 230507 (2013).

[2] P. Facchi, D. A. Lidar, and S. Pascazio, Physical Review A **69**, 032314 (2004); F. F. Fanchini, J. E. M. Hornos, and R. d. J. Napolitano, Physical Review A **75**, 022329 (2007).

[3] D. A. Golter, T. K. Baldwin, and H. Wang, Physical Review Letters **113**, 237601 (2014).

[4] J.-M. Cai, B. Naydenov, R. Pfeiffer, L. P. McGuinness, K. D. Jahnke, F. Jelezko, M. B. Plenio, and A. Retzker, New Journal of Physics **14**, 113023 (2012).

[5] M. Hirose, C. D. Aiello, and P. Cappellaro, Physical Review A **86**, 062320 (2012).

[6] J. Cai, F. Jelezko, N. Katz, A. Retzker, and M. B. Plenio, New Journal of Physics **14**, 093030 (2012).

[7] M. F. Riedel, P. Bhi, Y. Li, T. W. Hnsch, A. Sinatra, and P. Treutlein, Nature **464**, 1170 (2010); C. Gross, T. Zibold, E. Nicklas, J. Estve, and M. K. Oberthaler, Nature **464**, 1165 (2010).

[8] F. Gerbier, A. Widera, S. Flling, O. Mandel, and I. Bloch, Physical Review A **73**, 041602 (2006).

[9] M. Kitagawa and M. Ueda, Physical Review A **47**, 5138 (1993).

[10] I. D. Leroux, M. H. Schleier-Smith, and V. Vuleti, Physical Review Letters **104**, 073602 (2010).

[11] Y. Liu, S. Jung, S. E. Maxwell, L. D. Turner, E. Tiesinga, and P. D. Lett, Physical Review Letters **102**, 125301 (2009).

[12] G. A. Smith, S. Chaudhury, A. Silberfarb, I. H. Deutsch, and P. S. Jessen, Physical Review Letters **93**, 163602 (2004); G. A. Smith, A. Silberfarb, I. H. Deutsch, and P. S. Jessen, Physical Review Letters **97**, 180403 (2006).

[13] S. Chaudhury, G. A. Smith, K. Schulz, and P. S. Jessen, Physical Review Letters **96**, 043001 (2006).

[14] A. Kuzmich, L. Mandel, J. Janis, Y. E. Young, R. Ejnisman, and N. P. Bigelow, Physical Review A **60**, 2346 (1999); A. Kuzmich, L. Mandel, and N. P. Bigelow, Physical Review Letters **85**, 1594 (2000).

[15] G. I. Martone, Physical Review Letters **117** (2016), 10.1103/PhysRevLett.117.125301.

[16] H. J. Lipkin, N. Meshkov, and A. J. Glick, Nuclear Physics **62**, 188 (1965).

[17] W. Muessel, H. Strobel, D. Linnemann, T. Zibold, B. Juli-Daz, and M. K. Oberthaler, Phys. Rev. A **92**, 023603 (2015).

[18] N. Lundblad and I. B. Spielman, Physical Review Letters **118**, xxxxxx (2017).

[19] A. Messiah, *Quantum mechanics*, Vol. 2 (North-Holland, 1962).

[20] A. A. Wood, L. M. Bennie, A. Duong, M. Jasperse, L. D. Turner, and R. P. Anderson, Physical Review A **92**, 053604 (2015).

[21] M. Jasperse, M. J. Kewming, S. N. Fischer, P. Pakkiam, R. P. Anderson, and L. D. Turner, arXiv:1705.10965 (2017).

[22] A. Wood, L. Turner, and R. Anderson, Physical Review A **94**, 052503 (2016).

[23] The maximum Larmor frequency and thus static magnetic field we can detect Faraday rotation at is limited by the bandwidth of the detector.

[24] N. Ramsey, *Molecular beams* (Clarendon Press, 1956).